δf Simulation Studies of the Ion-Electron Two-Stream Instability in IBX*

Hong Qin, Ronald C. Davidson, and Edward A. Startsev
Plasma Physics Laboratory, Princeton University, Princeton, NJ 08543, USA

Abstract

The ion-electron two-stream instability is studied numerically for the high intensity heavy ion beams envisioned in the Integrated Beam Experiment (IBX). We consider a 1.7 MeV K^+ beam with 0.25 microcoulombs/m line density propagating through a small background electron population. The detailed linear properties of the ion-electron two-stream instability are studied using a 3D low-noise delta-f particle simulation method implemented in the Beam Equilibrium, Stability and Transport (BEST) code.

INTRODUCTION

In typical linear induction accelerators for heavy ion fusion drivers, the beam current is much higher than that in contemporary accelerators and storage rings in order to obtain sufficient fusion energy gain. For a given focusing lattice, most designs of heavy ion fusion drivers operate near the space-charge limit. Large space-charge forces inevitably induce a strong interaction among the beam particles, and in some regimes can result in collective instabilities [1, 2]. One of the major objectives in the Integrated Beam Experiment (IBX) proposed by the U.S. Heavy Ion Fusion Virtual National Laboratory is to study collective effects in a space-charge-dominated beam [3]. In particular, it is proposed to use IBX to investigate the ion-electron two-stream instability, which has been observed experimentally in high intensity accelerators and storage rings [4–6]. A well-documented example is the electron-proton (e-p) instability observed in the Proton Storage Ring experiment [4, 5]. Theoretical studies [1, 7–15] suggest that the relative streaming motion of the high-intensity beam particles through a background charge species provides the free energy to drive the classical *two-stream* instability, appropriately modified to include the effects of dc space charge, relativistic kinematics, presence of a conducting wall, etc. A background population of electrons can result by secondary emission when energetic beam ions strike the chamber wall [16–18], or through ionization of background neutral gas by the beam ions.

When electrons are present, two-stream interactions in IBX are expected to be stronger than the two-stream instabilities observed so far in proton machines because of the much larger beam intensity. In this paper, we study the ion-electron two-stream instability in IBX using a perturbative particle simulation method (δf method) for solving the Vlasov-Maxwell equations. As a low-noise nonlinear particle simulation technique, the δf method has been implemented in the recently developed Beam Equilibrium, Stability and Transport (BEST) code [19–21], which has been applied to a wide range of important collective processes in intense beams. We consider a K^+ IBX beam with $m = 39.1\,\mathrm{au}$ and kinetic energy $1.72\,\mathrm{MeV}$ in the low energy regime. Other beam parameters are: line density $N = 1.50 \times 10^{12}/\,\mathrm{m}$; RMS radius $R_b = 1.3\,\mathrm{cm}$; and beam transverse thermal speed $v_{th} = 0.054\beta_b c$. For the focusing lattice, the vacuum phase advance is $\sigma_v = 72^\circ$, and the applied betatron frequency is $\omega_{\beta b} = 1.21 \times 10^7\,\mathrm{s}^{-1}$.

δF SIMULATION METHOD

The theoretical model employed here is based on the nonlinear Vlasov-Maxwell equations. We consider a thin, continuous, high-intensity ion beam ($j = b$), with characteristic radius r_b propagating in the z-direction through background electrons ($j = e$), with each component described by a distribution function $f_j(\mathbf{x}, \mathbf{p}, t)$ [1, 7]. The nonlinear Vlasov-Maxwell equations for $f_j(\mathbf{x}, \mathbf{p}, t)$ and the self-generated fields can be approximated by [1, 7]

$$\left\{ \frac{\partial}{\partial t} + \mathbf{v} \cdot \frac{\partial}{\partial \mathbf{x}} - [\gamma_j \mathrm{m}_j \omega_{\beta j}^2 \mathbf{x}_\perp + e_j(\nabla\phi - \frac{v_z}{c}\nabla_\perp \mathrm{A}_z)] \cdot \frac{\partial}{\partial \mathbf{p}} \right\} f_j(\mathbf{x}, \mathbf{p}, t) = 0, \tag{1}$$

$$\nabla^2\phi = -4\pi \sum_j e_j \int d^3p f_j(\mathbf{x}, \mathbf{p}, t),$$
$$\nabla^2 A_z = -\frac{4\pi}{c} \sum_j e_j \int d^3p v_z f_j(\mathbf{x}, \mathbf{p}, t). \tag{2}$$

To solve the Vlasov-Maxwell equations, we use a low-noise δf method [19–21], where the total distribution function is divided into two parts, $f_j = f_{j0} + \delta f_j$. Here, $\omega_{\beta j}$ is the applied smooth-focusing frequency, f_{j0} is a *known* equilibrium solution ($\partial/\partial t = 0$) to the nonlinear Vlasov-Maxwell equations (1) and (2), and the numerical simulation is carried out to determine the detailed nonlinear evolution of the perturbed distribution function δf_j. This is accomplished by advancing the weight function defined by $w_j \equiv \delta f_j / f_j$, together with the particles' positions and momenta. The dynamical equations for w_{ji} is given by [21]

$$\frac{dw_{ji}}{dt} = -(1 - w_{ji}) \frac{1}{f_{j0}} \frac{\partial f_{j0}}{\partial \mathbf{p}} \cdot \delta\left(\frac{d\mathbf{p}_{ji}}{dt}\right),$$
$$\delta\left(\frac{d\mathbf{p}_{ji}}{dt}\right) \equiv -e_j \left(\nabla\delta\phi - \frac{v_{zji}}{c}\nabla_\perp \delta A_z\right), \tag{3}$$

* Research supported by the U.S. Department of Energy. We thank Drs. Ron Cohen, Christine Celata, Art Molvik, John Barnard, and Alex Freidman for many productive discussions.

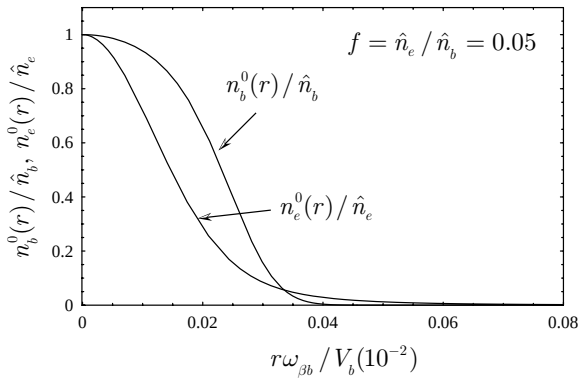

Figure 1: Normalized equilibrium beam ion and background electron density profiles.

where the subscript "ji" labels the i'th simulation particle of the j'th species, $\delta\phi = \phi - \phi_0$, and $\delta A_z = A_z - A_{z0}$. Here, the equilibrium solutions (ϕ_0, A_{z0}, f_{j0}) solve the steady-state Vlasov-Maxwell equations (1) and (2). A detailed description of the nonlinear δf method can be found in Ref. [21].

SIMULATION RESULTS

In the present simulations of the two-stream instability, instead of using the theoretically-convenient KV distribution [1], we assume that the background equilibrium distribution ($\partial/\partial t = 0$) is the more realistic *bi-Maxwellian* distribution with temperature $T_{j\perp} = const.$ in the transverse plane, and temperature $T_{j\parallel} = const.$ in the longitudinal direction. That is,

$$f_{j0}(r,\mathbf{p}) = \frac{\hat{n}_j}{(2\pi m_j)^{3/2}\gamma_j^{5/2}T_{j\perp}T_{j\parallel}^{1/2}} \times \exp\left\{-\frac{(p_z-\gamma_j m_j\beta_j c)^2}{2\gamma_j^3 m_j T_{j\parallel}} - \frac{p_\perp^2/2\gamma_j m_j}{T_{j\perp}}\right\} \times \exp\left\{-\frac{\gamma_j m_j\omega_{\beta j}^2 r^2/2 + e_j(\phi_0-\beta_j A_{z0})}{T_{j\perp}}\right\}, \quad (4)$$

where $\hat{n}_j$ is the density on axis ($r = 0$) of the j'th species, and ϕ_0 and A_{z0} are the equilibrium self-field potentials, determined self-consistently from the nonlinear Maxwell equations

$$\frac{1}{r}\frac{\partial}{\partial r}r\frac{\partial\phi_0(r)}{\partial r} = -4\pi\sum_j e_j\int d^3p f_{j0}(r,\mathbf{p}), \quad (5)$$
$$\frac{1}{r}\frac{\partial}{\partial r}r\frac{\partial A_{z0}(r)}{\partial r} = -\frac{4\pi}{c}\sum_j e_j\int d^3p v_z f_{j0}(r,\mathbf{p}).$$

The equilibrium density profile for the each species, $n_j^0(r)/\hat{n}_j = (1/\hat{n}_j)\int d^3p f_{j0}(r,\mathbf{p},t)$ $(j = b,e)$, can be readily obtained once the equilibrium potentials ϕ_0 and A_{z0} are determined numerically from Eqs. (4) and (5). If the beam particles are the only species in the system, the equilibrium can be be characterized by a single dimensionless parameter $s_b \equiv \hat{\omega}_{pb}^2/2\gamma_b^2\omega_{\beta b}^2$, where $\hat{\omega}_{pb}^2 = 4\pi\hat{n}_b e_b^2/m_b\gamma_b$ is the beam plasma frequency on axis. The parameter s_b, which measures the self-field intensity relative to the applied focusing force, satisfies $0 \le s_b \le 1$, with $s_b = 0$ corresponding to the zero space-charge limit, and $s_b \to 1$ to the space-charge-dominated limit. For IBX, we take $s_b = 0.996$, and the density profile is close to a flat-top profile, because s_b is very close to the space-charge dorminated limit. If there is a small background electron population, the space-charge force will be partially neutralized, and the beam density profile relaxes to a bell-shape. Plotted in Fig. 1 are the density profiles for an ion-electron two-species equilibrium with fractional charge neutralization $f \equiv \hat{n}_e/\hat{n}_b = 0.05$, and $V_e = 0$ and $\omega_{\beta e} = 0$ for stationary background electrons.

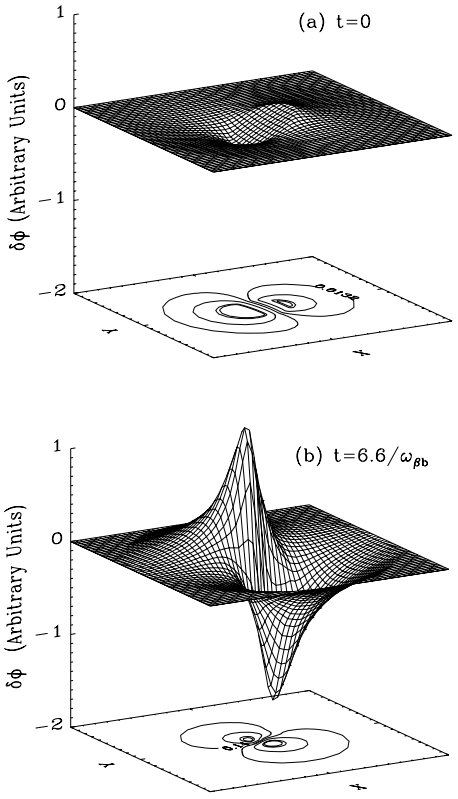

Figure 2: The x-y projection (at fixed value of z) of the perturbed electrostatic potential $\delta\phi(x,y,t)$ for the ion-electron two-stream instability growing from a small initial perturbation, shown at (a) $t = 0$, and (b) $\omega_{\beta b}t = 6.6$.

To simulate the ion-electron two-stream instability , we perturb the two-species equilibrium discussed above with a small initial perturbation, and use the *linearized* version of the BEST code to simulate the dynamics of the system for many thousands of wave periods. In Fig. 2, the $x-y$ projection of the perturbed potential $\delta\phi$ at a fixed longitudinal position is plotted at $t = 0$ and $t = 6.6/\omega_{\beta b}$. Clearly, $\delta\phi$ grows to a moderate amplitude by $t = 6.6/\omega_{\beta b}$, and

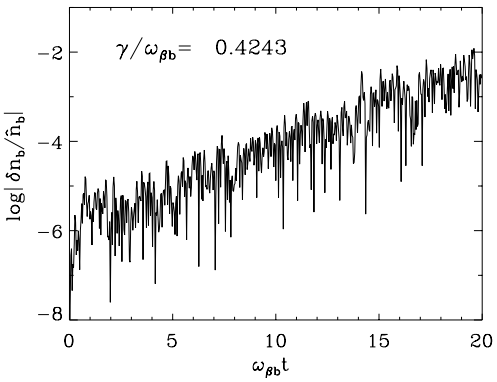

Figure 3: Time history of pertubed desnity $\delta n_b/\hat{n}_b$ at a fixed spatial location.

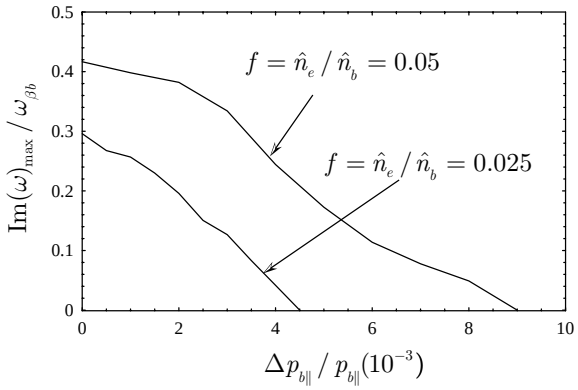

Figure 4: The maximum linear growth rate $(\mathrm{Im}\,\omega)_{max}$ of the ion-electron two-stream instability decreases as the longitudinal momentum spread of the beam ions increases.

the $l = 1$ dipole mode is the dominant unstable mode, for which the growth rate is measured to be $\mathrm{Im}\,\omega = 0.42\omega_{\beta b}$. Plotted in Fig. 3 is the time history of the beam density perturbation at one spatial location. Evidently, after an initial transition period, the perturbation grows exponentially, which is the expected behavior of an instability during the linear growth phase.

In the simulation results for the two-stream instability presented above, we have assumed initially cold beam ions in the longitudinal direction ($\Delta p_{b\|}/p_{b\|} = 0$) to maximize the growth rate of the instability. Here, $p_{b\|} = \gamma_b m_b V_b$. In general, when the longitudinal momentum spread of the beam ions is finite, Landau damping by parallel ion kinetic effects provides a mechanism that reduces the growth rate. Shown in Fig. 4 is a plot of the maximum linear growth rate $(Im\omega)_{max}$ versus the normalized initial axial momentum spread $\Delta p_{b\|}/p_{b\|}$ obtained in the numerical simulations for the cases where $f \equiv \hat{n}_e/\hat{n}_b = 5\%$ and $f = 2.5\%$. As evident from Fig. 4, the growth rate decreases dramatically as $\Delta p_{b\|}/p_{b\|}$ is increased. When $\Delta p_{b\|}/p_{b\|}$ is high enough, the mode is completely stabilized by longitudinal Landau damping effects by the beam ions. This result agrees qualitatively with theoretical predications [9]. For a fixed value of $\Delta p_{b\|}/p_{b\|}$, the growth rate obtained from the simulation is several times smaller than the theoretical value predicted by the dispersion relation derived for a KV beam with flat-top density profile [7, 8]. This difference can be attributed to the fact that the present simulations are carried out for more realistic thermal equilibrium beams with bell-shape density profiles. The nonlinear space-charge potential due to the bell-shape density profiles induces substantial tune spread in the transverse direction, which provides an additional damping mechanism, and reduces the growth rate of the two-stream instability [20].

REFERENCES

[1] R. C. Davidson and H. Qin, *Physics of Intense Charged Particle Beams in High Energy Accelerators* (World Scientific, 2001).

[2] A. W. Chao, *Physics of Collective Beam Instabilities in High Energy Accelerators* (Wiley, NewYork, 1993).

[3] J. J. Barnard et al., Laser and Particle Beams **21**, in press (2003).

[4] D. Neuffer et al., Nucl. Instr. Methods Phys. Res. **A321**, 1 (1992).

[5] R. J. Macek et al., in *Proc. 2001 Particle Accelerator Conference*, pp. 668–672 (2001).

[6] M. Giovannozzi, E. Mtral, G. Mtral, G. Rumolo and F. Zimmermann, Phys. Rev. ST Accel. Beams **6**, 010101 (2003).

[7] R. C. Davidson, H. Qin, P. H. Stoltz and T. S. Wang, Phys. Rev. ST Accel. Beams. **2**, 054401 (1999).

[8] R. C. Davidson, H. Qin and T. S. Wang, Physics Letters A **252**, 213 (1999).

[9] R. C. Davidson and H. Qin, Phys. Lett.**A 270**, 177 (2000).

[10] T.-S. F. Wang, P. J. Channell, R. J. Macek and R. C. Davidson, Phys. Rev. ST Accel. Beams **6**, 014204 (2003).

[11] P. J. Channell, Phys. Rev. ST Accel. Beams **5**, 114401 (2003).

[12] K. Ohmi, T. Toyama and C. Ohmori, Phys. Rev. ST Accel. Beams **5**, 114402 (2002).

[13] D. G. Koshkarev and P. R. Zenkevich, Particle Accelerators **3**, 1 (1972).

[14] E. Keil and B. Zotter, CERN-ISH-TH/71-58, Technical report, CERN (1971).

[15] L. J. Laslett, A. M. Sessler and D. Möhl, Nucl. Instr. Methods Phys. Res. **121**, 517 (1974).

[16] R. H. Cohen et al., in *Proc. 2003 Particle Accelerator Conference* (2003).

[17] A. W. Molvik et al., in *Proc. 2003 Particle Accelerator Conference* (2003).

[18] M. T. F. Pivi and M. A. Furman, Phys. Rev. ST Accel. Beams **6**, 034201 (2003).

[19] H. Qin, E. A. Startsev, R. C. Davidson and W. W. Lee, Laser and Particle Beams **21**, 1 (2003).

[20] H. Qin, E. A. Startsev and R. C. Davidson, Phys. Rev. ST Accel. Beams **6**, 014401 (2003).

[21] H. Qin, R. C. Davidson and W. W. Lee, Phys. Rev. ST Accel. and Beams **3**, 084401 (2000).